

Instabilities of laser beams counterpropagating through a Brillouin-active medium

Paul Narum,* Alexander L. Gaeta, Mark D. Skeldon, and Robert W. Boyd

The Institute of Optics, University of Rochester, Rochester, New York 14627

Received September 8, 1987; accepted October 21, 1987

Counterpropagating laser beams in a Brillouin-active medium are shown to become unstable to the growth of amplitude and phase fluctuations. Slightly above threshold, the nature of the instability is the temporal growth of sidemodes separated from the laser frequency by approximately the Brillouin frequency of the medium. This process leads to sinusoidal oscillations of the intensities of the transmitted waves. At higher input intensities the system can become chaotic; many sidemodes are excited, and the transmitted fields fluctuate wildly. The origin of the Brillouin instability is the combined action of the gain of the standard stimulated Brillouin scattering (SBS) process and of the coupling of the waves due to multiwave mixing mediated by the electrostrictive interaction. The threshold for the instability is at least several times lower than the threshold of the standard SBS process involving a single pump beam.

INTRODUCTION

One of the simplest processes in nonlinear optics is the mutual interaction of two light waves in a nonlinear medium. Despite its conceptual simplicity, several recent theoretical investigations have shown that this interaction can lead to very complicated behavior, including chaotic fluctuations of the intensities of the transmitted waves. The possibility of instability in the interaction of counterpropagating waves was considered by Silberberg and Bar-Joseph¹ for the case of a medium with a Kerr nonlinearity having a noninstantaneous response. They showed that for sufficiently large input intensities the transmitted fields fluctuate in time and that at high input intensities these fluctuations become chaotic. The origin of this instability is the combined action of the gain experienced by the sidemodes to the input fields and of the distributed feedback due to scattering from the grating formed by the interference between the two input fields. More recently, Gaeta *et al.*² have shown that chaotic temporal fluctuations can occur in the polarizations of counterpropagating waves in a polarization-sensitive Kerr medium and that this instability can occur even for the case of a medium with instantaneous response.

In this paper we treat the stability of counterpropagating waves in a Brillouin-active medium. It is known from studies of stimulated Brillouin scattering (SBS)³ and Brillouin-enhanced four-wave mixing⁴⁻⁷ that the Brillouin interaction leads to strong coupling among the interacting waves. The great strength of this coupling suggests that instabilities can occur readily in this system. In fact, Randall and Albritton⁸ have shown that very complicated periodic and chaotic behavior can occur for the different geometry in which a reflective boundary is placed at one end of a Brillouin-active medium and a single laser field is applied. In addition, periodic oscillations in the intensities have been predicted and observed⁹ for the case of SBS in an optical fiber placed between two reflective mirrors. Moreover, Zel'dovich and Shkunov¹⁰ and Andreev *et al.*¹¹ have predicted that, in the limit of a medium short enough so that phase-mismatch

effects can be ignored, counterpropagating waves can be unstable to the growth of sidemodes at the Brillouin frequency. Narum and Boyd⁷ have briefly discussed this same instability for a medium of arbitrary length in the context of Brillouin-enhanced four-wave mixing.

THEORETICAL DEVELOPMENT

We assume that the total optical field within the Brillouin-active medium can be represented as the sum of the forward- and backward-traveling plane-wave components as

$$E_{\text{TOT}}(z, t) = \frac{1}{2}E_f(z, t)\exp[i(kz - \omega t)] + \frac{1}{2}E_b(z, t)\exp[i(-kz - \omega t)] + \text{c.c.} \quad (1)$$

Owing to the process of electrostriction, the local density of the medium is modified by the total optical field in accordance with the linearized acoustic wave equation³:

$$\frac{\partial^2 \bar{\rho}}{\partial t^2} - \Gamma' \frac{\partial}{\partial t} \frac{\partial^2 \bar{\rho}}{\partial z^2} - v^2 \frac{\partial^2 \bar{\rho}}{\partial z^2} = \frac{-\gamma}{8\pi} \frac{\partial^2}{\partial z^2} E_{\text{TOT}}^2, \quad (2)$$

where $\bar{\rho}$ denotes the variation of the density from its mean value ρ_0 , $\Gamma' = 4\eta/3\rho_0$ is a damping parameter, η characterizes the viscosity, v is the speed of sound in the medium, and γ is the electrostrictive constant. In evaluating the electrostrictive driving term on the right-hand side of Eq. (2), we drop those contributions that oscillate at optical frequencies. We also assume that the optical fields obey the slowly varying amplitude approximation in that $|\partial E_j/\partial z| \ll |kE_j|$ for j equal to f and b , in which case the right-hand side of Eq. (2) becomes

$$\frac{q^2 \gamma}{16\pi} (E_f E_b^* e^{iqz} + \text{c.c.}),$$

with $q = 2k$. The form of Eq. (2) can now be simplified by introducing the complex representation

$$\bar{\rho} = \frac{1}{2}\rho(z, t)e^{iqz} + \text{c.c.}, \quad (3)$$

making the slowly varying amplitude approximation for the phonon field, and assuming that the phonons are strongly damped, i.e., $\Gamma|\partial\rho/\partial t| \gg (2\Omega^2/q)|\partial\rho/\partial z|$, to give

$$\frac{\partial^2\rho}{\partial t^2} + \Gamma\frac{\partial\rho}{\partial t} + \Omega^2\rho = \frac{q^2\gamma}{8\pi}E_fE_b^*, \quad (4)$$

where $\Gamma = \Gamma'q^2$ denotes the Brillouin linewidth and $\Omega = qv$ denotes the Brillouin frequency. We now assume that the dielectric constant of the medium has a contribution proportional to the material density, in which case the nonlinear (NL) polarization can be expressed as

$$P^{\text{NL}}(z, t) = \frac{\gamma}{4\pi\rho_0}\tilde{\rho}(z, t)E_{\text{TOT}}(z, t). \quad (5)$$

We substitute P^{NL} and E_{TOT} into the driven wave equation and get

$$\frac{\partial^2 E_{\text{TOT}}}{\partial z^2} - \frac{1}{(c/n)^2}\frac{\partial^2 E_{\text{TOT}}}{\partial t^2} = \frac{4\pi}{c^2}\frac{\partial^2 P^{\text{NL}}}{\partial t^2}, \quad (6)$$

where n is the refractive index of the medium. We then use Eq. (1), make the slowly varying amplitude approximation, and thereby obtain the coupled amplitude equations for the forward- and backward-traveling waves:

$$\frac{\partial E_f}{\partial z} + \frac{1}{(c/n)}\frac{\partial E_f}{\partial t} = i\kappa\rho E_b, \quad (7a)$$

$$\frac{\partial E_b}{\partial z} - \frac{1}{(c/n)}\frac{\partial E_b}{\partial t} = -i\kappa\rho^* E_f, \quad (7b)$$

where $\kappa = \gamma\omega/4\rho_0nc$. Equations (4) and (7) have been derived previously⁸ but were used to treat the case in which E_b was generated by reflection of the transmitted field E_f . We impose different boundary conditions, namely, we treat the case in which both E_f and E_b are applied externally. As we show below, complex temporal behavior can occur even when there is no external feedback. Equations (4) and (7) yield the following simple steady-state solution (designated by the superscript zero):

$$\rho^0(z) = \frac{\gamma}{8\pi v^2}E_f^0(z)E_b^{0*}(z), \quad (8a)$$

$$E_f^0(z) = E_f^0(0)\exp\left(ig_0\frac{\Gamma}{\Omega}I_b z\right), \quad (8b)$$

$$E_b^0(z) = E_b^0(L)\exp\left[ig_0\frac{\Gamma}{\Omega}I_f(L-z)\right], \quad (8c)$$

where $g_0 = \gamma^2\omega^2/2\Gamma nvc^3\rho_0$ is the line-center Brillouin amplitude gain coefficient and $I_f^0 = (nc/8\pi)|E_f(0)|^2$ and $I_b^0 = (nc/8\pi)|E_b(L)|^2$ are the input intensities of each wave. The threshold for the usual single-beam SBS process is usually taken as the condition that g_0IL be equal to 15, but we show in the next section that the threshold for the Brillouin instability treated here is typically considerably lower. We see from Eqs. (8) that in the steady state the fields do not exchange energy but that the phase velocity of propagation of each wave is affected by the intensity of the other wave. The NL contribution to the phase shift is proportional to the ratio Γ/Ω of the Brillouin linewidth to the Brillouin frequency shift.

LINEAR STABILITY ANALYSIS

To determine the stability characteristics of the steady-state solution [Eq. (8)], we perturb the amplitudes of the forward and backward waves such that

$$E_f = E_f^0 + f_s(z)e^{\lambda t} + f_a(z)\exp(\lambda^*t), \quad (9a)$$

$$E_b = E_b^0 + b_s(z)e^{\lambda t} + b_a(z)\exp(\lambda^*t), \quad (9b)$$

where the second and third terms represent small perturbations to the steady-state solution. If $\text{Re } \lambda > 0$, the steady-state solution will be temporally unstable to the growth of these perturbations. We now insert these expressions for the electric fields into Eqs. (4) and (7) and derive the linearized equations for the perturbation amplitudes:

$$\frac{df_s}{dz} = (-\lambda n/c + gI_b^0)f_s + ig_0\frac{\Gamma}{\Omega}\left(\frac{cn}{8\pi}E_f^0E_b^{0*}\right)b_s + g\left(\frac{cn}{8\pi}E_f^0E_b^0\right)b_a^*, \quad (10a)$$

$$\frac{db_s}{dz} = (\lambda n/c - gI_f^0)b_s - ig_0\frac{\Gamma}{\Omega}\left(\frac{cn}{8\pi}E_f^{0*}E_b^0\right)f_s - g\left(\frac{cn}{8\pi}E_f^0E_b^0\right)f_a^*, \quad (10b)$$

$$\frac{df_a^*}{dz} = -(\lambda n/c + gI_b^0)f_a^* - ig_0\frac{\Gamma}{\Omega}\left(\frac{cn}{8\pi}E_f^{0*}E_b^0\right)b_a^* - g\left(\frac{cn}{8\pi}E_f^0E_b^{0*}\right)b_s, \quad (10c)$$

$$\frac{db_a^*}{dz} = (\lambda n/c + gI_f^0)b_a^* + ig_0\frac{\Gamma}{\Omega}\left(\frac{cn}{8\pi}E_f^0E_b^0\right)f_a^* + g\left(\frac{cn}{8\pi}E_f^{0*}E_b^{0*}\right)f_s, \quad (10d)$$

where

$$g = g_0\frac{i\Gamma\Omega}{\lambda^2 + \Gamma\lambda + \Omega^2}. \quad (10e)$$

To understand the nature of the coupling described by these equations, we assume that $\text{Im } \lambda > 0$. [Because λ and λ^* of Eqs. (9) form a complex-conjugate pair, we can always require λ to have this property.] We can then interpret f_s and b_s to be the amplitudes of the forward- and backward-traveling Stokes fields, respectively, and f_a and b_a to be the amplitudes of the forward- and backward-traveling anti-Stokes fields, respectively. Then, for example, Eq. (10a) describes the spatial evolution of the forward-traveling Stokes wave. The first term on the right-hand side describes the change in the propagation vector that is associated with λ and with the normal SBS gain (proportional to g) owing to the presence of the backward pump wave. From Eq. (10e) we can see that the gain coefficient g is resonantly enhanced when $\text{Im } \lambda$ (i.e., the frequency difference between the pump and Stokes fields) is equal to the Brillouin frequency Ω . The second term in Eq. (10a) can be interpreted as the scattering of the backward-Stokes wave from the refractive index variation associated with the standing-wave pattern created by the interference of the counterpropagating pump waves. This term describes distributed feedback of the same type as that discussed by Silberberg and Bar-

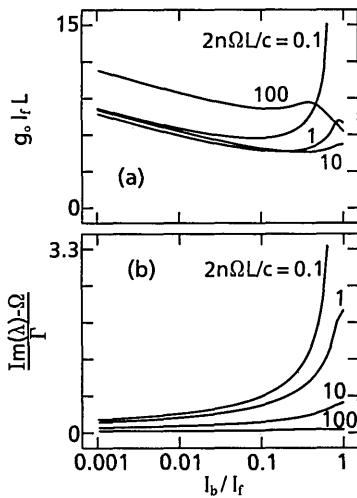


Fig. 1. Forward input intensity at (a) the threshold for instability and (b) the frequency of oscillation, each plotted as a function of the backward-to-forward input intensities for $\Gamma/\Omega = 0.03$ and for various values of the normalized length of the medium $2n\Omega L/c$.

Joseph.¹ The third term describes the four-wave mixing process arising from the scattering of the backward pump wave from the retreating acoustic wave driven by the interference between the forward pump wave and the backward anti-Stokes wave. The other equations [(10b)–(10d)] can be interpreted in an analogous fashion. For each equation the second term vanishes for the case of a sharp Brillouin line, $\Gamma/\Omega \rightarrow 0$, which is the limit in which SBS is usually studied. In this limit the system of four coupled equations decouples into two systems of two coupled equations; each system describes a four-wave mixing process.¹⁰

We solve the linearized equations [Eqs. (10)] with pump wave amplitudes given by Eqs. (8b) and (8c) by seeking solutions for the perturbations that vary as $\exp(\alpha z)$. The general solution for $f_s, b_s, f_a,$ and b_a is then found in terms of linear combinations of such solutions for each of the four eigenvalues of α . The particular solution is found by applying the boundary conditions $f_s(0) = b_s(L) = f_a(0) = b_a(L) = 0$. Because the steady-state solution is unstable for $\text{Re } \lambda > 0$, we find the threshold for instability by setting $\text{Re } \lambda = 0$. More than one solution to the linearized equations can be found even under these conditions, and the different solutions correspond to different longitudinal modes of the system and to different oscillation frequencies $\text{Im } \lambda$. The instability threshold for the system is the lowest intensity that yields a solution to the coupled linearized equations with $\text{Re } \lambda = 0$ for any value of $\text{Im } \lambda$.

Typical results of the stability analysis are shown in Fig. 1 for the case of a Brillouin medium with $\Gamma/\Omega = 0.03$. In Fig. 1(a) the normalized forward input intensity at threshold for the Brillouin instability is plotted as a function of the ratio of the input intensities for several different values of the normalized length of the medium. In each case the system is unstable in the region above the curve. Figure 1(b) shows the normalized oscillation frequency $\text{Im } \lambda$ at threshold. The oscillation frequency is close to the Brillouin frequency for each case shown. The quantity $2n\Omega L/c$, which we call the normalized length of the medium, is therefore approximately equal to the single-pass phase mismatch ΔkL of the nearly degenerate four-wave mixing process.⁷ The threshold input

intensity increases rapidly for a short medium ($2n\Omega L/c = 0.1$) with balanced pumping ($I_b/I_f = 1$). This increase occurs because for balanced pumping the Stokes gain is equal to the anti-Stokes loss, and for a short medium the coupling between the waves is sufficiently strong to prevent either wave from growing.^{10,12,13} For comparison, we have plotted in Fig. 2 the results of the stability analysis for the case of a medium with a much larger Brillouin linewidth such that $\Gamma/\Omega = 0.3$. Although these two cases are quite similar in their behavior near the threshold for instability, we will show below that for sufficiently large input intensities the instability becomes chaotic for the case of $\Gamma/\Omega = 0.3$.

The Brillouin instability predicted above is an example of a dynamic instability in that the perturbation to the steady-state solution grows exponentially in time and will thus develop from an arbitrarily small initial perturbation. The process usually known as SBS is the exponential *spatial* growth of an input Stokes wave and hence is not a dynamic instability. Even if no Stokes wave is applied externally, an input Stokes (and anti-Stokes) wave is created by spontaneous Brillouin scattering, that is, scattering from thermally generated phonons. The threshold for SBS excited by a single laser beam and seeded by spontaneous Brillouin scattering is described by the condition that the single-pass amplitude gain $g_0 I_f L$ is approximately equal to 15. We see from Figs. 1 and 2 that the threshold for the Brillouin instability is lower than the threshold for single-beam SBS for most of the cases that we consider; hence the dynamic (Brillouin) instability will occur but SBS will not. However, the threshold for instability predicted in Figs. 1 and 2 is higher than that of single-beam SBS for the case of a short medium with balanced pumping and for the case of a long medium with imbalanced pumping. To determine whether SBS or the dynamic instability will occur in these two cases, a more detailed consideration of the initiation of SBS by spontaneous scattering must be performed. The effects of spontaneous Brillouin scattering on the present calculation can be accounted for in an approximate manner by modifying the boundary conditions for the perturbations so that the input fields acquire nonzero values. For the case of highly imbalanced pumping, the physical situation is similar to that of

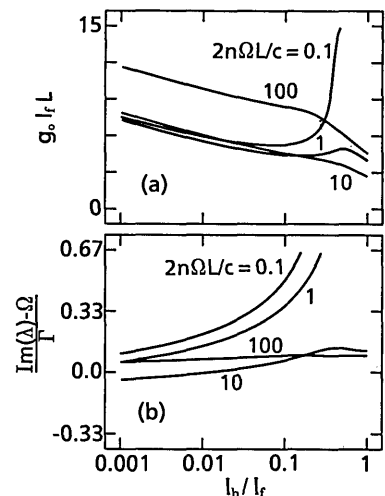


Fig. 2. Same as in Fig. 1 but for the case of a much larger Brillouin linewidth such that $\Gamma/\Omega = 0.3$.

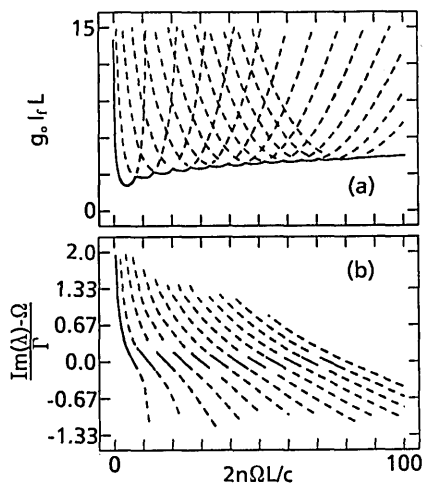


Fig. 3. Forward input intensity at (a) the threshold for instability and (b) the frequency of oscillation for each longitudinal mode of the system. The forward input intensity is plotted as a function of the normalized length of the medium for the case of equal input intensities and $\Gamma/\Omega = 0.3$. The solid curve in (a) gives the lowest threshold intensity for any mode, and the solid curves in (b) give the corresponding oscillation frequency.

SBS with a single pump beam, and a threshold for SBS is simply $gIL = 15$, where I is the intensity of the stronger pump beam. Therefore, since in this limit the dynamic instability treated here has a higher threshold, it is probably not observable experimentally for this case. For the case of a short medium ($2n\Omega L/c \ll 1$) with balanced pumping, the situation is quite different. Here, as mentioned above, the coupling between the Stokes wave (which, in the absence of coupling, experiences gain) and the anti-Stokes wave (which, in the absence of coupling, experiences loss) is so large that the coupled solution experiences little net gain, and, as a result, even the usual SBS process is suppressed by the presence of counterpropagating pump waves.¹⁰ To see that even the normal SBS gain is suppressed by the presence of the counterpropagating pump wave, we consider the simple limiting case in which Γ/Ω approaches 0 and the Stokes and anti-Stokes waves are tuned exactly to the Brillouin resonance. By solving Eqs. (10a) and (10d), we find that the transmitted Stokes field strength is related to the input Stokes and anti-Stokes fields when $I_f = I_b$ and in the limit $gI_f L \gg 1$ by

$$f_s(L) = 2f_s(0) + b_a^*(L). \quad (11)$$

Hence, in the presence of counterpropagating pump waves, the Stokes field is amplified only by a factor of approximately 2, although the amplification in the presence of a single pump wave of the same intensity would be $\exp(gI_f L)$, where $gI_f L$ was assumed to be large.

In Fig. 3 we have plotted the normalized length of the medium versus the normalized input intensity $g_0 I_f L$ [Fig. 3(a)] and normalized oscillation frequency $(\text{Im} \lambda - \Omega)/\Gamma$ [Fig. 3(b)] corresponding to each of the allowed solutions of the linearized perturbation Eqs. (10) with $\text{Re} \lambda = 0$. We assume the case $\Gamma/\Omega = 0.3$ and balanced pumping ($I_b/I_f = 1$). The various U-shaped curves in Fig. 3(a) can be interpreted as the threshold for instability for the different longitudinal modes of the system. The solid curve in Fig. 3(a) corresponds to the lowest input intensity that leads to instability

for any mode. Local minima in this threshold occur for $2n\Omega L/c$ approximately equal to integral multiples of π . The solid curves in Fig. 3(b) give the oscillation frequency of the mode with the lowest threshold. This frequency is approximately equal to the Brillouin frequency except for the case of a short medium, in which case the lowest-frequency mode of the system has an eigenfrequency much greater than the Brillouin frequency.

Silberberg and Bar-Joseph¹⁴ have shown that the origin of the instability of counterpropagating waves in a Kerr medium with noninstantaneous response is the combined action of the gain experienced by the sidemodes of the pump frequency and distributed feedback. Distributed feedback¹⁵ results from the scattering of light at the sidemode frequencies from the grating induced by the interference between the two pump waves. However, this gain-distributed feedback mechanism does not appear to be the origin of the instability for the case of a Brillouin-active medium. The Brillouin instability occurs even in the limit of a medium with a sharp Brillouin linewidth, although, as mentioned above, there is no distributed feedback structure in this limit. The Brillouin instability appears to be more closely related to the infinite reflectivity that is predicted to occur for certain values of the pump intensity in phase conjugation by four-wave mixing. We can establish this connection most simply by considering the limit $\Gamma/\Omega \rightarrow 0$, in which case the linearized perturbation equations [Eqs. (10)] decouple into two sets of equations. Each set describes a four-wave mixing process. These equations are identical to those describing Brillouin-enhanced four-wave mixing, and the Brillouin instability is a consequence of the infinite reflectivity that can occur in phase conjugation by Brillouin-enhanced four-wave mixing.⁷ Infinite reflectivity is also predicted for

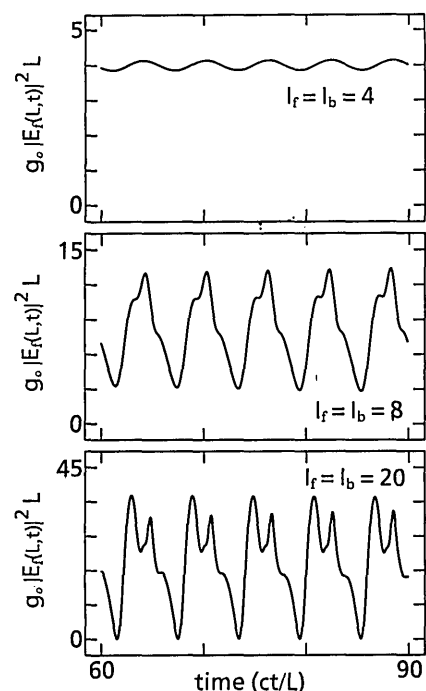


Fig. 4. Temporal evolution of the transmitted intensity of the forward-traveling wave for the case $2n\Omega L/c = 2$, $\Gamma/\Omega = 0.03$, and equal input intensities. For all input intensities shown, the output oscillates periodically with a fundamental frequency equal to the Brillouin frequency.

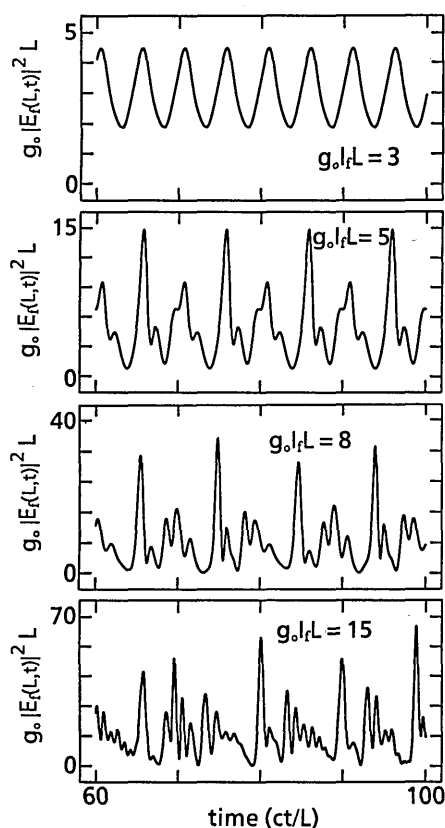


Fig. 5. Temporal evolution of the transmitted intensity of the forward-traveling wave for the case $2n\Omega L/c = 2$, $\Gamma/\Omega = 0.3$, and equal input intensities. As the input intensities are increased, the system becomes chaotic following the period-doubling route. For input intensities such that $g_o I_f L = 3$, the output oscillates with a fundamental frequency equal to the Brillouin frequency. For input intensities $g_o I_f L = 5$ and $g_o I_f L = 8$ the output oscillates with a fundamental frequency equal to one half and one quarter, respectively, of the Brillouin frequency. For $g_o I_f L = 15$ the temporal evolution is chaotic.

phase conjugation by degenerate four-wave mixing in a Kerr medium,¹⁶ and it might be thought that this infinite reflectivity is related to the instabilities that can occur with counterpropagating beams in a Kerr medium.^{1,2} However, in the scalar limit such instabilities occur only for the case of a medium with noninstantaneous response, whereas the infinite phase-conjugate reflectivity is predicted for any value of the medium response time. Infinite reflectivity in degenerate four-wave mixing in the phase-conjugation geometry does not necessarily imply instabilities in counterpropagating waves for the following reason: When the angle between the pump and probe waves in the phase-conjugation geometry becomes sufficiently small, additional nearly phase-matched contributions to the nonlinear polarization, known as cross-coupled waves, become important.¹⁷ These additional contributions prevent the development of the instability unless the medium has a noninstantaneous response. Curiously (and importantly), the cross-coupled waves do not contribute for the case of a Brillouin-active medium with $\Gamma \ll \Omega$ because these additional contributions are not Brillouin resonant. Moreover, polarization instabilities in counterpropagating waves have been shown theoretically to exist even for a medium with instantaneous response,² and a related instability has been observed experimentally.¹⁸

NUMERICAL EVALUATION OF THE COUPLED NONLINEAR EQUATIONS

To determine the full dynamic behavior of the system above the threshold for instability, we have numerically integrated the coupled nonlinear equations [Eqs. (4)–(7)] in both space and time by using the method of characteristics. In performing the numerical integration, we ramp on the input fields slowly starting at time $t = 0$ to simulate the turn-on characteristics of the laser. We display the results of these calculations in Figs. 4 and 5 over a time interval that begins 60 transit times after time $t = 0$. At this time the temporal evolution is no longer dominated by transient effects associated with the turn on of the laser. Figure 4 shows the temporal evolution of the output intensity of the forward-traveling wave for several different values of the input intensity when $\Gamma/\Omega = 0.03$ and $2n\Omega L/c = 2$ and for equal input intensities. In each case shown the output oscillates periodically with a fundamental frequency approximately equal to the Brillouin frequency.

Results of the numerical calculation for the same conditions as those of Fig. 4, except assuming the case of a broader Brillouin line ($\Gamma/\Omega = 0.3$), are shown in Fig. 5. For this case of a broader Brillouin linewidth, the output displays chaotic fluctuations for sufficiently large input intensities. The system evolves from a stable state to a chaotic state as the input intensities are increased following the period-doubling route. For input intensities slightly above the threshold for instability ($g_o I_f L = 3$), the transmitted intensity oscillates at the Brillouin frequency. However, for the higher input intensity $g_o I_f L = 5$, the output intensity oscillates periodically with a fundamental frequency equal to one half of the Brillouin frequency. For still higher intensities ($g_o I_f L = 8$), the output intensity oscillates with a fundamental frequency equal to one quarter of the Brillouin frequency. At the highest intensity shown ($g_o I_f L = 15$), the output intensity fluctuates in a chaotic fashion. We have verified that the output is chaotic in the strict sense by using the method of Grassberger and Procaccia.¹⁹

CONCLUSIONS

We have demonstrated that counterpropagating waves in a Brillouin-active medium are temporally unstable above a certain threshold intensity. We have also shown how the threshold for instability varies as a function of the ratio between the input intensities I_b/I_f for various values of the wave-vector mismatch, which is proportional to $2n\Omega L/c$. We have found that even when one of the beams is relatively weak, the instability can occur at a threshold intensity much lower than that normally required for single-beam SBS involving only the stronger wave. The temporal evolution immediately above this threshold is periodic and at higher intensities can, for the case of a relatively broad Brillouin linewidth, become chaotic.

ACKNOWLEDGMENTS

This work was supported by the sponsors of the New York State Center for Advanced Optical Technology and by the U.S. Army Research Office. Robert W. Boyd is grateful to the Norwegian Defence Research Establishment for their hospitality.

*Present address, Norwegian Defence Research Establishment, Kjeller, Norway.

REFERENCES

1. Y. Silberberg and I. Bar-Joseph, *Phys. Rev. Lett.* **48**, 1541 (1982).
2. A. L. Gaeta, R. W. Boyd, J. R. Ackerhalt, and P. W. Milonni, *Phys. Rev. Lett.* **58**, 2432 (1987).
3. W. Kaiser and M. Maier, in *Laser Handbook 2*, F. T. Arrechi and E. O. Schulz-Dubois, eds. (North-Holland, Amsterdam, 1972), p. 1078.
4. N. F. Andreev, V. I. Bespalov, A. M. Kiselev, A. Z. Matveev, G. A. Pasmanik, and A. A. Shilov, *Sov. Phys. JETP Lett.* **32**, 625 (1980).
5. A. M. Scott, *Opt. Commun.* **45**, 127 (1983).
6. M. D. Skeldon, P. Narum, and R. W. Boyd, *Opt. Lett.* **12**, 343 (1987).
7. P. Narum and R. W. Boyd, *IEEE J. Quantum Electron.* **QE-23**, 1211 (1987).
8. C. J. Randall and J. R. Albritton, *Phys. Rev. Lett.* **52**, 1887 (1984).
9. I. Bar-Joseph, A. A. Friesem, E. Lichtman, and R. G. Waarts, *J. Opt. Soc. Am. B* **2**, 1606 (1985).
10. B. Ya Zel'dovich and V. V. Shkunov, *Sov. J. Quantum Electron.* **12**, 223 (1982).
11. N. F. Andreev, V. I. Bespalov, A. M. Kiselev, G. A. Pasmanik, and A. A. Shilov, *Sov. Phys. JETP* **55**, 612 (1982).
12. N. Bloembergen, *Nonlinear Optics* (Benjamin, New York, 1965), p. 115.
13. R. W. Boyd, M. G. Raymer, P. Narum, and D. J. Harter, *Phys. Rev. A* **24**, 411 (1981).
14. Y. Silberberg and I. Bar-Joseph, *J. Opt. Soc. Am. B* **1**, 662 (1984).
15. H. Kogelnik and C. V. Shank, *J. Appl. Phys.* **43**, 2327 (1972).
16. A. Yariv and D. M. Pepper, *Opt. Lett.* **1**, 16 (1977).
17. J. H. Marburger, in *Optical Phase Conjugation*, R. A. Fisher, ed. (Academic, New York, 1983), Chap. 4, p. 121.
18. D. M. Pepper, D. Fekete, and A. Yariv, *Appl. Phys. Lett.* **33**, 41 (1978).
19. P. Grassberger and I. Procaccia, *Phys. Rev. Lett.* **50**, 346 (1983).